Proceedings of the 17th World Congress
The International Federation of Automatic Control
Seoul, Korea, July 6-11, 2008

Model Predictive Control of glucose concentration in subjects with type 1 diabetes: an in silico trial

L. Magni [*,1] **D. M. Raimondo** [*] **C. Dalla Man** [**]
G. De Nicolao [*] **B. Kovatchev** [***] **C. Cobelli** [**]

[*] *Dipartimento di Informatica e Sistemistica, University of Pavia, via Ferrata 1, I-27100 Pavia, Italy*
[**] *Department of Information Engineering, University of Padova, Via Gradenigo 6/B, I-35131 Padova, Italy*
[***] *University of Virginia Health System Box 800137 Charlottesville, VA 22908, USA*

Abstract: The feedback control of glucose concentration in type 1 diabetic patients using subcutaneous insulin delivery and subcutaneous continuous glucose monitoring is considered. A recently developed in-silico model of glucose metabolism is employed to generate virtual patients on which control algorithms can be validated against interindividual variability. An in silico trial consisting of 100 patients is used to assess the performances of a linear output feedback model predictive controller, designed on the basis of the in-silico model. More than satisfactory results are obtained in the great majority of virtual patients. The experiments highlight the crucial role of the anticipative feedforward action driven by the meal announcement information. Preliminary results indicate that further improvements may be achieved by means of a nonlinear model predictive control scheme.

1. INTRODUCTION

The automated control of normoglycemia in subjects with type 1 diabetes, also called artificial pancreas, has been subject of extensive research since the 1970s Bequette (1998), Hovorka (2005). However, the first devices, e.g. the Biostator^{TM}, which used intravenous (*i.v.*) *BG* sampling and *i.v.* insulin and glucose delivery, were cumbersome and unsuited for outpatient use. A minimally-invasive closed-loop system using subcutaneous (*s.c.*) continuous glucose monitoring and *s.c.* insulin pump delivery was needed. To date, several *s.c.* − *s.c.* systems, have been tested Hovorka (2005), Klonoff (2007). From a control viewpoint, the main challenges are time delays, constraints, meal disturbances, and nonlinear dynamics. Most of the control schemes proposed in literature are based on either *PID* (Proportional Integral Derivative) or *MPC* (Model Predictive Control) control laws, see e.g. Panteleon et al. (2006), Hovorka (2005), Dua et al. (2006). Due to the presence of significant delays in the glucose metabolism model, a well designed feedforward action able to consider in advance a meal announcement signal is essential in order to guarantee satisfactory performances. Within *MPC*, feedforward and feedback control actions are jointly designed and constraints are taken into account in a very natural way. The recent advancements in nonlinear *MPC*, see e.g. Mayne et al. (2000), and the development of a new generation of models of glucose metabolism make this control technique even more promising.

The need of guaranteeing parameter identificability from easily measurable experimental data motivated the development of parsimonious models of glucose metabolism see e.g. the classical minimal model Bergmann et al. (1979). By contrast, in silico large-scale simulation models aim to describe the glucose-insulin system in as much detail as possible. The major limitation of most in silico models is that they were validated on few subjects and only by means of plasma concentration measurements. Recently, a new-generation in silico model has been developed taking advantage of the availability of a unique-meal data set of 204 nondiabetic individuals Dalla Man et al. (2007). The subjects underwent a triple tracer meal protocol, making it possible to obtain in a virtually model-independent fashion the time course of all the relevant glucose and insulin fluxes during a meal. Thus, by using a "concentration and flux" portrait, it was possible to model the glucose-insulin system by resorting to a sub-system forcing function strategy which minimizes structural uncertainties in modeling the various unit processes.

In this paper, the above model is used to randomly generate virtual diabetic patients. Suitable modifications are introduced to reflect the absence of endogenous insulin secretion, while the parameter variability in the original dataset is used to model interindividual variability of the diabetic population. Validating algorithms on a whole set of different patients (in silico trial) is the only realistic

[1] Corresponding author: L. Magni (lalo.magni@unipv.it)
E-mail addresses: D. M. Raimondo (davide.raimondo@unipv.it)
C. Dalla Man (chiara.dallaman@dei.unipd.it)
G. De Nicolao giuseppe.denicolao@unipv.it
C. Cobelli (cobelli@dei.unipd.it)
B. Kovatchev (boris@virginia.edu)
The authors acknowledge the financial support by the Juvenile Diabetes Research Foundation 'Artificial Pancreas Project' at the University of Virginia.

way of addressing robustness of the artificial pancreas in the face of interindividual variability so as to maximize success chances in the subsequent clinical trials conducted on real patients.

In the present work, the in silico model is used to design a linear output feedback MPC scheme which is then tested on an in silico trial consisting of 100 synthetic type I diabetic subjects "followed" for 4 days, receiving breakfast, lunch, and dinner each day. The overall results, as measured by several established performance indices, are more than satisfactory for the great majority of virtual patients. It is highlighted the role of the feedforward action that takes advantage of the meal announcement information. Moreover, the controller performances are shown to be robust with respect to errors in the meal announcement signal. Finally, in order to improve the glucose concentration regulation of the (few) not well regulated patients, a preliminary test is carried out by using a nonlinear state-feedback MPC scheme. A definite improvement of performances is observed, indicating that nonlinear MPC has the potential for achieving very effective glucose concentration control.

2. VIRTUAL PATIENTS

In order to synthesize and test the controller, we used the meal glucose-insulin model Dalla Man et al. (2007). Some modifications have been introduced in order to simulate the metabolic specifics of T1DM (see Magni et al. (2007)).

Glucose intestinal absorption Glucose intestinal absorption is modeled by a recently developed three-compartment model

$$\begin{aligned} Q_{sto}(t) &= Q_{sto_1}(t) + Q_{sto_2}(t) \\ \dot{Q}_{sto_1}(t) &= -k_{gri} Q_{sto_1}(t) + d(t) \\ \dot{Q}_{sto_2}(t) &= -k_{gut}(t, Q_{sto}) Q_{sto2}(t) + k_{gri} Q_{sto_1}(t) \\ \dot{Q}_{gut}(t) &= -k_{abs} Q_{gut}(t) + k_{gut}(t, Q_{sto}) Q_{sto2}(t) \\ Ra(t) &= \frac{f k_{abs} Q_{gut}(t)}{BW} \end{aligned}$$

where $Q_{sto}(mg)$ is amount of glucose in the stomach (solid, Q_{sto_1}, and liquid phase, Q_{sto_2}), $Q_{gut}(mg)$ glucose mass in the intestine, k_{gri} rate of grinding, k_{abs} rate constant of intestinal absorption, f fraction of intestinal absorption which actually appears in plasma, $d(mg/min)$ amount of ingested glucose, $BW(Kg)$ body weight and Ra $(mg/kg/min)$ glucose rate of appearance in plasma, k_{gut} rate constant of gastric emptying which is a time-varying nonlinear function of Q_{sto}

$$\begin{aligned} &k_{gut}(t, Q_{sto}) = k_{\min} + \tfrac{k_{\max} - k_{\min}}{2} \left\{ \tanh\left[\alpha\left(Q_{sto} - b\bar{D}(t)\right)\right] \right. \\ &\left. - \tanh\left[\beta\left(Q_{sto} - d\bar{D}(t)\right)\right] + 2 \right\} \\ &\alpha = \tfrac{5}{2\bar{D}(t)(1-b)}, \beta = \tfrac{5}{2\bar{D}(t)d}, \ \bar{D}(t) = Q_{sto}(\bar{t}) + \textstyle\int_{\bar{t}}^{\bar{t}_f} d(\bar{\tau}) d\tau \end{aligned}$$

where $\bar{t}$ and $\bar{t}_f$ are the initial and final times of the last ingestion, while b, d, k_{max} and k_{min} are model parameters.

Glucose subsystem A two-compartment model is used to describe glucose kinetics

$$\begin{aligned} \dot{G}_p(t) &= EGP(t) + Ra(t) - U_{ii} - E(t) \\ &\quad -k_1 G_p(t) + k_2 G_t(t) \\ \dot{G}_t(t) &= -U_{id}(t) + k_1 G_p(t) - k_2 G_t(t) \end{aligned}$$

where G_p (mg/kg) and G_t (mg/kg) are glucose in plasma and rapidly-equilibrating tissues, and in slowly-equilibrating tissues, respectively, EGP endogenous glucose production $(mg/kg/min)$, E $(mg/kg/min)$ renal excretion, U_{ii} and U_{id} insulin-independent and -dependent glucose utilizations, respectively $(mg/kg/min)$, and k_1 and k_2 rate parameters. The insulin-independent glucose utilizations U_{ii} is assumed constant.

Glucose Renal Excretion Renal excretion, which occurs if plasma glucose exceeds a certain threshold, can be modeled as follows

$$E(t) = \begin{cases} k_{e_1}\left[G_p(t) - k_{e_2}\right] & if\ G_p(t) > k_{e_2} \\ 0 & if\ G_p(t) \le k_{e_2} \end{cases}$$

where k_{e_1} is glomerular filtration rate and k_{e_2} renal threshold of glucose.

Endogenous Glucose Production EGP comprises a direct glucose signal and a delayed insulin signal

$$EGP(t) = \max\left\{0, k_{p1} - k_{p2} G_p(t) - k_{p3} I_d(t)\right\}$$

where the delayed insulin signal I_d $(pmol/l)$ is given by

$$\begin{aligned} \dot{I}_1(t) &= -k_i\left[I_1(t) - I(t)\right] \\ \dot{I}_d(t) &= -k_i\left[I_d(t) - I_1(t)\right] \end{aligned}$$

with $I(pmol/l)$ the plasma insulin concentration, k_{p1} the extrapolated EGP at zero glucose and insulin, k_{p2} liver glucose effectiveness, k_{p3} parameter governing amplitude of insulin action on the liver, and k_i rate parameter accounting for delay between insulin signal and insulin action.

Glucose Utilization Glucose utilization is made up of two components: the insulin independent one U_{ii}, which represents the glucose uptake by the brain and erythrocytes, and the insulin dependent component U_{id}, which depends nonlinearly on glucose in the tissues

$$\begin{aligned} U_{id}(t) &= \tfrac{V_m(t) G_t(t)}{K_m + G_t(t)},\ V_m(t) = V_{m0} + V_{mx} X(t) \\ \dot{X}(t) &= -p_{2U} X(t) + p_{2U}\left[I(t) - I_b\right] \end{aligned}$$

where K_m, V_{m0}, V_{mx} are model parameters, X $(pmol/l)$ is the remote insulin signal, I_b $(pmol/l)$ is the basal insulin level and p_{2U} is rate constant of insulin action on the peripheral glucose utilization.

Subcutaneous insulin kinetics The present paper adopts a variation of a model described in Verdonk et al. (1981)

$$\begin{aligned} \dot{S}_1(t) &= -(k_{a1} + k_d) S_1(t) + u(t) \\ \dot{S}_2(t) &= k_d S_1(t) - k_{a2} S_2(t) \end{aligned}$$

where $u(t)$ $(pmol/kg/min)$ represents administration (bolus and infusion) of insulin. The first compartment represents the amount of the nonmonomeric insulin in the subcutaneous space, which is partly transformed in monomeric insulin (second compartment) and partly enters the circulation with rate constants of insulin absorption k_d and k_{a1} respectively; the monomeric insulin is finally absorbed with rate constant k_{a2}.

Insulin subsystem The model equations are

$$\begin{aligned} \dot{I}_l(t) &= -\left(m_1 + m_3\right) I_l(t) + m_2 I_p(t) \\ \dot{I}_p(t) &= -\left(m_2 + m_4\right) I_p(t) + m_1 I_l(t) + k_{a1} S_1(t) \\ &\quad + k_{a2} S_2(t) \end{aligned}$$

where $I_p(t) = V_I I(t)$ $(pmol/kg)$ and I_l $(pmol/kg)$ are insulin masses in plasma and in liver, respectively, V_I (l/kg) being the body weight normalized insulin volume and m_i, $i = 1, ..., 4$ are model parameters.

Subcutaneous glucose kinetics Subcutaneous glucose concentration G_M (mg/dl) is obtained as

$$\dot{G}_M(t) = -k_{sc}G_M(t) + k_{sc}\frac{G_p(t)}{V_G}$$

where V_G (dl/kg) is the body weight normalized glucose volume and k_{sc} is a rate constant.

Virtual patient generation In order to obtain parameter joint distributions in type 1 diabetes, the parameter identified in 204 subjects in health were used as starting point Dalla Man et al. (2007). Some modification was needed to realistically describe a type 1 diabetic subject: basal glucose concentration was assumed to be on average 50 mg/dl higher than in subjects in health; steady state insulin concentration (due to an external insulin pump) was assumed to be on average four times higher than in subjects in health; basal endogenous glucose production was assumed to be 35% higher than in subjects in health, and steady state insulin clearance was assumed to be one third lower than in subjects in health; parameters relating to insulin action on both glucose production and utilization were assumed to one third lower than in subjects in health. For all these parameters/variable the same inter-subject variability found in subjects in health was maintained. The parameters were assumed to be log-normal distributed to guarantee that they were always positive, thus covariance matrix (26×26) was calculated using the log-transformed parameters. 100 subjects were generated using the joint distribution, i.e. 100 realization of the log-transformed parameter vector were randomly extracted from the multivariate normal distribution with mean equal to mean of the log-transformed parameters and 26×26 covariance matrix. Finally, the parameters in the 100 in silico subjects were obtained by antitransformation.

3. MODEL PREDICTIVE CONTROL

The glucose metabolism model can be rewritten in the following compact way

$$\begin{aligned} \dot{x}(t) &= f(t, x(t), u(t), d(t)) \\ y(t) &= G_M(t) \end{aligned}$$

where $x = [Q_{sto_1}, Q_{sto_2}, Q_{gut}, G_p, G_t, I_p, X, I_1, I_d, I_l,\ S_1, S_2,\ G_M]$, and $f(\cdot,\cdot,\cdot,\cdot)$ is derived from the model equations reported in Section 2. The system is subject to the following constraints

$$x_{\min} \leq x \leq x_{\max} \tag{1}$$

$$u_{\min} \leq u \leq u_{\max} \tag{2}$$

where $x_{\min}$, $x_{\max}$, $u_{\min}$ and $u_{\max}$ denote lower and upper bounds on the state and input respectively. Typically, they represent limits on the glucose concentration and on the insulin delivery rate. In the following, it is assumed that meal announcement is available, i.e. the disturbance signal (the meal) is known in advance.

The MPC control law (Mayne et al. (2000), Camacho and Bordons (2004), Maciejowski (2001)) is based on the solution of a Finite Horizon Optimal Control Problem $(FHOCP)$, where a cost function $J(\bar{x}, u)$ is minimized with respect to the input u subject to the state dynamics of a model of the system, and to state- and input-constraints. Letting u^o be the solution of the $FHOCP$, according to the Receding Horizon paradigm, the feedback control law $u = \kappa^{MPC}(x)$ is obtained by applying to the system only the first part of the optimal solution. In this way, a closed-loop control strategy is obtained solving an open-loop optimization problem.

MPC control laws can be formulated for both discrete- and continuous-time systems. In this paper, a discrete-time Linear MPC $(LMPC)$ is derived from an input-output linearized approximation of the full model. Moreover, a state-feedback nonlinear MPC $(NMPC)$ scheme is derived that exploits the full nonlinear model.

3.1 Unconstrained Linear Model Predictive Control

Given the basal values of G_p, G_t, and I_p that are characteristic of each patient, the associated equilibrium point with $D = 0$ is called $(\bar{x}, \bar{u}, \bar{d})$. Around this equilibrium point, assuming $k_{gut}(t, Q_{sto}) = (k_{\max} - k_{\min})/2$, the system is linearized and discretized with sample time T_s yielding

$$\begin{aligned} x(k+1) &= A_D x(k) + B_{Du}u(k) + B_{Dd}d(k) \\ y(k) &= C_D x(k) \end{aligned}$$

After a model order reduction step the following transfer function representation is obtained

$$Y(z) = \frac{N_U(z)}{DE(z)}U(z) + \frac{N_D(z)}{DE(z)}D(z) \tag{3}$$

with

$$\begin{aligned} N_U(z) &= b_{n-1}z^{n-1} + ... + b_0 \\ DE(z) &= z^n + a_{n-1}z^{n-1} + a_{n-2}z^{n-2} + ... + a_0 \\ N_D(z) &= b_{Dn-1}z^{n-1} + ... + b_{D0} \end{aligned}$$

Since the two transfer functions have the same denominator, the following input-output representation is obtained

$$\begin{aligned} & y(k+1) \\ = & -a_{n-1}y(k) - a_{n-2}y(k-1) - ... - a_0 y(k-n+1) \\ & +b_{n-1}u(k) + ... + b_0 u(k-n+1) \\ & +b_{Dn-1}d(k) + ... + b_{D0}d(k-n+1) \end{aligned}$$

Finally, system (3) can be given the following state-space (nonminimal) representation

$$\begin{aligned} x_{IO}(k+1) &= A_{IO}x_{IO}(k) + B_{IO}u(k) + M_{IO}d(k) \\ y(k) &= C_{IO}x_{IO}(k) \end{aligned}$$

where $x_{IO}(k+1) = [y(k+1)', ..., y(k-n+2)', u(k)', ..., u(k-n+2)', d(k)', ..., d(k-n+2)']'$ and the matrices A_{IO}, B_{IO}, M_{IO}, C_{IO} are defined accordingly.

In order to derive the $LMPC$ control law the following quadratic discrete-time cost function is considered

$$\begin{aligned} & J(x_{IO}(k), u(\cdot)) \\ = & \sum_{i=0}^{N-1} \left(\left\| y^0(k+i) - y(k+i) \right\|^2_{Q_D} + \left\| u(k+i) \right\|^2_{R_D} \right) \\ & + \left\| y^0(k+N) - y(k+N) \right\|^2_{S_D} \end{aligned}$$

where N is the prediction horizon, $y^o(k)$ the desired output at time k and $Q_D = Q_D' \geq 0$, $R_D = R_D' > 0$, $S_D = S_D' \geq 0$ symmetric matrices.

The evolution of the system can be re-written in a compact way as follows

$$Y(k) = \mathcal{A}_c x_{IO}(k) + \mathcal{B}_c U(k) + \mathcal{M}_c D(k)$$

where $Y(k) = [y(k+1), y(k+2), ..., y(k+N-1), y(k+N)]$, $D(k) = [d(k)', d(k+1)', ..., d(k+N-1)', d(k+N)']'$, $U(k) = [u(k)', u(k+1)', ..., u(k+N-1)', u(k+N)']'$ and

$\mathcal{A}_c$, $\mathcal{B}_c$, $\mathcal{M}_c$, are derived using the discrete time Lagrange formula

$$\begin{aligned} x_{IO}(k+i) &= A_{IO}^{i} x_{IO}(k) \\ &\quad + \sum_{j=0}^{i-1} A_{IO}^{i-j-1} \left(B_{IO} u(k+j) + M_{IO} d(k+j)\right) \end{aligned}$$

In this way, letting $Y^o(k) = [y^o(k+1)', y^o(k+2)', ..., y^o(k+N-1)', y^o(k+N)']'$ the cost function becomes

$$\begin{aligned} &\bar{J}(x(k), u(\cdot)) \\ &= \left(Y^o(k) - Y(k)\right)' \mathcal{Q} \left(Y^o(k) - Y(k)\right) + U'(k) \mathcal{R} U(k) \\ &= \left(Y^o(k) - \mathcal{A}_c x_{IO}(k) - \mathcal{B}_c U(k) - \mathcal{M}_c D(k)\right)' \mathcal{Q} \\ &\quad * \left(Y^o(k) - \mathcal{A}_c x_{IO}(k) - \mathcal{B}_c U(k) - \mathcal{M}_c D(k)\right) \\ &\quad + U'(k) \mathcal{R} U(k) \end{aligned}$$

where $\mathcal{Q}$ and $\mathcal{R}$ are block-diagonal matrices that contain the matrices Q, R and S. In the unconstrained case, the solution of the optimization problem is

$$\begin{aligned} U^o(k) &= \left(\mathcal{B}_c' \mathcal{Q} \mathcal{B}_c' + \mathcal{R}\right)^{-1} \mathcal{B}_c' \\ &\quad * \mathcal{Q} \left(Y^o(k) - \mathcal{A}_c x_{IO}(k) - \mathcal{M}_c D(k)\right) \end{aligned}$$

where the future values of the set point and the disturbance signal (meal) are considered. Finally, following the Receding Horizon approach the control law is given by

$$u^o(k) = [\, I \; 0 \; \ldots \; 0 \,] \, U^o(k)$$

In view of the input constraints (2), only a saturated value will be applied to the system. The satisfaction of the state constraints, on the contrary, cannot be guaranteed; it is only possible to tune parameters Q, R, S and N to improve the regulation performance. The major advantages of this input-output $LMPC$ scheme are that an observer is not required (x_{IO} includes past input and output values only), and that it is very easily implementable because on-line optimization is avoided.

3.2 Constrained Linear Model Predictive Control

With a relatively small increase of the computational burden it is possible to consider explicitly both input and state constraints by solving a constrained linear quadratic optimization problem. This can be done by solving on-line a quadratic programming problem or by using an explicit solution derived through a multiparametric approach. In this paper the results obtained with constrained $LMPC$ are not reported because they did not show any significant improvement. In fact, the explicit consideration of only input constraints does not improve the performance of the unconstrained saturated control law, while the fully constrained problem, i.e. also with state constraints, introduces nontrivial problems due to the approximation error caused by linearization and model reduction. Further work is required to explore this approach.

3.3 Nonlinear Model Predictive Control

The potentiality of a full nonlinear approach were explored by considering a state-feedback nonlinear MPC where the following continuous time cost function is used

$$\begin{aligned} &J(\bar{x}, u(\cdot), \bar{t}) \\ &= \int_{t=\bar{t}}^{\bar{t}+L} \left(y^0(\tau) - y(\tau)\right)' Q \left(y^0(\tau) - y(\tau)\right) \\ &\quad + \left(u(\tau) - \bar{u}\right)' R \left(u(\tau) - \bar{u}\right) d\tau \end{aligned}$$

In order to develop a full hybrid solution, the control input $u(\tau)$ is constrained to be piecewise constant, see Magni and Scattolini (2004). Both input and state constraints are explicitly considered.

4. PERFORMANCE ASSESSMENT

Virtual protocol The performance of closed-loop glucose control was tested on a 4-day virtual protocol:

- the simulation starts in basal steady-state and the first meal is the dinner at 7.30 pm of Day 1;
- the patient has breakfast at time 9.30 am with 45g of glucose, lunch at 13.30 with 75g of glucose and dinner at 7.30 pm within 85g of glucose;
- in the first part of the simulation the patient has a subcutaneous bolus based on an open-loop strategy, while at 9.30 pm of day 2 the controller is plugged in.

Performances indices Some established indices of glucose control were considered.

(1) Low Blood Glucose Index ($LBGI$) Kovatchev et al. (2005): Given n samples of the glucose mass in the plasma $G_p(i)$

$$LBGI = \frac{1}{n} \sum_{i=1}^{n} rl(G_p(i)/V_G)$$

where $rl(\cdot) = 10 * \left(g \left(\ln(\cdot)^a - b\right)\right)^2$ if $g \left(\ln(\cdot)^a - b\right) < 0$ and zero otherwise. The parameters g, a and b are equal to 24.7159, 0.3043 and 1.6156 respectively. This index captures the propensity of the algorithm to overshoot the target and eventually trigger hypoglycemia.

(2) High Blood glucose index ($HBGI$) Kovatchev et al. (2005): Directly linked with $LBGI$ it captures the propensity of the algorithm to stay above the target range

$$HBGI = \frac{1}{n} \sum_{i=1}^{n} rh(G_p(i)/V_G)$$

where $rh(\cdot) = 10 * \left(g \left(\ln(\cdot)^a - b\right)\right)^2$ if $g \left(\ln(\cdot)^a - b\right) > 0$ and zero otherwise.

(3) Percent of time spent below the lower bound of the target range ($PERCL$): the target range is defined as 90 $mg/dl \leq G_p/V_G \leq 180$ mg/dl; percent of time is computed on a 1 minute basis over the considered simulation interval.

(4) Percent of time spent over the upper bound of the target range ($PERCH$).

(5) Minimum of blood glucose concentration G_p/V_G (Min_Glycemia).

(6) Maximum of blood glucose concentration G_p/V_G (Max_Glycemia).

In order to allow for the transition from open-loop to closed-loop regulation all the indices are computed for two different periods: *commutation* since 9.30 pm of day 2 to 6.30 am of day 3 and *regulation* after 6.30 am of day 3.

5. RESULTS

Experiment 1 The ingested amount of glucose is exactly the one considered in the protocol. 100 subjects are simulated using an $LMPC$ control law synthesized with $T_s = 30$ min, $n = 2$, $N = 8$, $R_D = 1$ and $Q_D = S_D = q$,

where q has been tuned for each subject and the set point is taken equal to 135 mg/dl. For a more detailed analysis of the effect of q on the performance see Magni et al. (2007)).

Experiment 2 The ingested amount of glucose is randomly varied within $\pm 40\%$ of the nominal value for all 100 patients. The $LMPC$ control law has the same parameters as those used for Experiment 1 and relies on the nominal glucose dose to decide the feedforward action.

Experiment 3 The amount of ingested glucose is the same as in Experiment 2 for all 100 patients, but the $LMPC$ control law is applied without meal announcement.

Experiment 4 In order to explore the potentiality of $NMPC$, some virtual patients undergoing Experiment 1 were also controlled by means of an $NMPC$ scheme with set point 135 mg/dl. The following constraints were imposed on glucose plasma concentration and external insulin: $G_p/V_G > 90\ mg/dl$, $0 \leq u \leq 150U/h$. In the cost function $L = 4h$, $R = 1$, and Q was tuned for each subject.

Experiments evaluation Figure 1 shows the scatter plot of the Min_Glycemia and Max_Glycemia during *regulation* for Experiments 1-3. Figure 2 shows the plasma glucose and external insulin evolution in Subject 3. Nominal and real meals are reported in the bottom panel. In Figure 3 the boxplots for indices 1-4 are reported for Experiments 1-3 during both *commutation* ("*c*") and *regulation* ("*r*") periods. In Fig. 4, the $LMPC$ and $NMPC$ are compared in Subjects 88 and 36 showing plasma glucose and external insulin evolution.

The vertical black lines in Fig. 2 and 4 represent the beginning and the end of the *commutation* period.

With reference to the *regulation* period, it is apparent from Figs. 1 and 3 that during Experiment 1 no hypoglycemic events occurred. In fact, the minimum value of Glycemia is always greater than 90 mg/dl. Conversely, in some subjects the maximum value is rather high but only episodically for short time periods after meal. In fact, the values of the index $HBGI$, reported in Figure 3, are not excessively high (note that $HBGI \simeq 10$ with $G_p = 190\ mg/dl$). As evident from Figure 2, the controller normalizes Glycemia very quickly even starting from unfavorable initial conditions. The transient of the external insulin and the meal plot show that the insulin flux increase anticipates the meal when meal announcement is used. Imperfect knowledge of the amount of ingested glucose (Experiment 2) causes an only marginal deterioration of performance of the regulator, while the results obtained with Experiment 3 show the benefit of meal announcement, see Figs. 1-3. As shown in Fig. 4 for Subjects 88 and 36, the adoption of an $NMPC$ scheme, in place of an $LMPC$ one, can bring substantial improvement with respect to the prevention of hypo- and hyper-glycemic events. The advantage of the nonlinear predictive control scheme is twofold: constraints on Glycemia are explicitly allowed for and knowledge of the nonlinear dynamics is exploited.

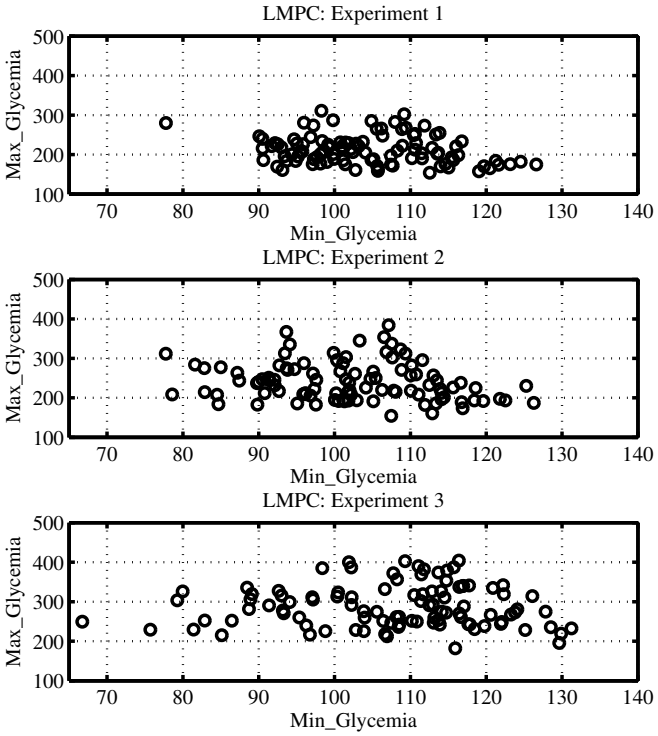

Fig. 1. Minimum versus maximum value during *regulation*

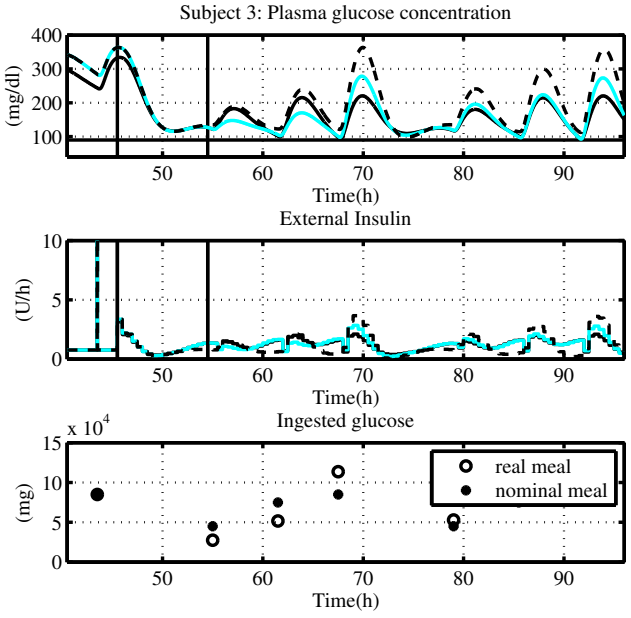

Fig. 2. Subject 3: Experiment 1 (continuous), Experiment 2 (grey), Experiment 3 (dashed)

6. CONCLUSIONS

The in silico trial has demonstrated that linear output feedback MPC achieves satisfactory Glycemia regulation in a population of 100 type 1 diabetic patients. Preliminary tests conducted in some virtual patients have shown that

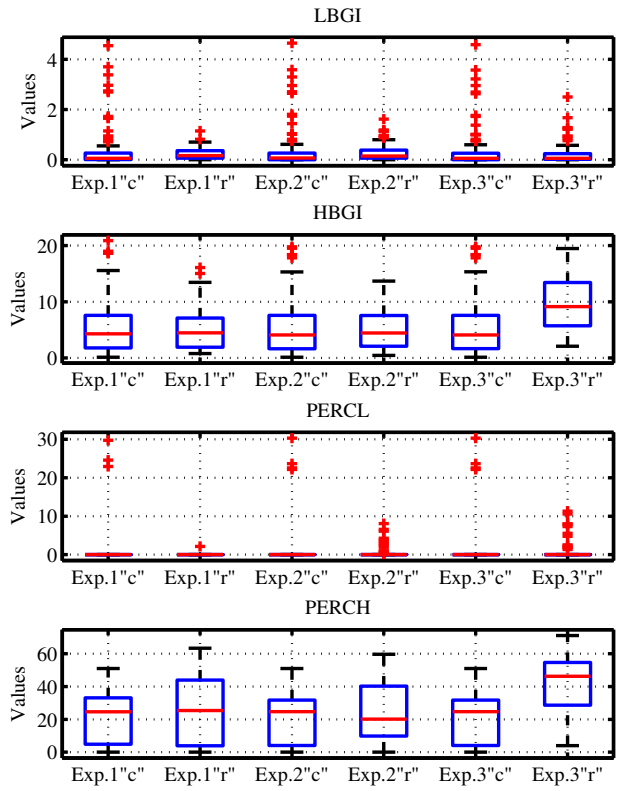

Fig. 3. Boxplot of the indices for the Experiments 1-3 during *commutation* and *regulation* respectively

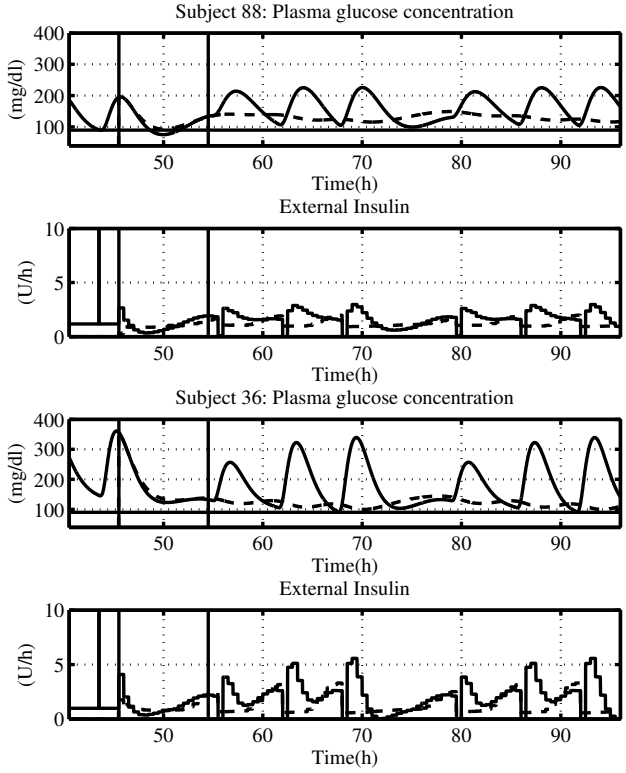

Fig. 4. Subjects 1 and 2: Experiment 1 ($LMPC$ - continuous) and Experiment 4 ($NMPC$ - dashed)

state-feedback $NMPC$ has the potential to introduce further improvements. The proposed scheme is also robust with respect to noise in the meal announcement signal. Robustness in the face of sensor errors could be investigated by complementing the simulator with a probabilistic model of the sensor noise. Another research direction concerns the development of state observers to be used in conjunction with nonlinear MPC.

REFERENCES

B. W. Bequette. A critical assessment of algorithms and challanges in the development of a closed-loop artificial pancreas. *Diabetes Technology & Therapeutics*, 7:28–47, 1998.

R. N. Bergmann, Y. Z. Ider, C. R. Bowden, and C. Cobelli. Quantitative estimation of insulin sensitivity. *Am. J. Physiol.*, 236:E667–E677, 1979.

E. F. Camacho and C. Bordons. *Model Predictive Control*. Springer, 2004.

C. Dalla Man, R. A. Rizza, and C. Cobelli. Meal simulation model of the glucose-insulin system. *IEEE Transactions on Biomedical Engeneering*, page in press, 2007.

P. Dua, F. J. Doyle III, and E. N. Pistikopoulos. Model-based blood glucose control for type 1 diabetes via parametric programming. *IEEE Transactions on Biomedical Engineering*, 53:1478–1491, 2006.

R. Hovorka. Continuous glucose monitoring and closed-loop systems. *Diabetic Medicine*, 23:1–12, 2005.

D. C. Klonoff. The artificial pancreas: How sweet engineering will solve bitter problems. *J. of Diabetes Science and Technology*, 1:72–81, 2007.

B. P. Kovatchev, W. L. Clarke, M. Breton, K. Brayman, and A. McCall. Quantifying temporal glucose variability in diabetes via continuous glucose monitoring: Mathematical methods and clinical application. *Diabetes Technol Ther.*, 7:842–862, 2005.

J. Maciejowski. *Predictive Control with Constraints*. Prentice-Hall, 2001.

L. Magni and R. Scattolini. Model predictive control of continuous-time nonlinear systems with piecewise constant control. *IEEE Trans. on Automatic Control*, 49:900–906, 2004.

L. Magni, D. M. Raimondo, L. Bossi, C. Dalla Man, G. De Nicolao, B. Kovatchev, and C. Cobelli. Model predictive control of type 1 diabetes: An in silico trial. *Journal of Diabetes Science and Technology*, 1(6):804–812, 2007.

D. Q. Mayne, J. B. Rawlings, C. V. Rao, and P. O. M. Scokaert. Constrained model predictive control: Stability and optimality. *Automatica*, 36:789–814, 2000.

A. E. Panteleon, M. Loutseiko, G. M. Steil, and K. Rebrin. Evaluation of the effect of gain on the meal response of an automated closed-loop insulin delivery system. *Diabetes*, 55:1995–2000, 2006.

C. A. Verdonk, R. A Rizza, and J. E. Gerich. Effects of plasma glucose concentration on glucose utilization and glucose clearance in normal man. *Diabetes*, 30:535–537, 1981.